Industry Science and Engineering Vol. 2 No. 10, 2025

Academic Education Publishing House

Research on the Dynamic Characteristics of Pantographs Based on Cartesian Coordinates

Jie Yu[1], Qingjun Li[2], Jinfa Guan[3,*], Junqing Chen[3], Shuai Jiang[4]

[1]*Yangtze River Coastal Railway Group Sichuan Co., Ltd., Chengdu, Sichuan, China*

[2]*China Railway First Survey and Design Institute Group Co., Ltd., Xi'an, Shaanxi, China*

[3]*Southwest Jiaotong University, Chengdu, Sichuan, China*

[4]*Safety Technology Center, National Railway Administration, Beijing, China*

**Corresponding Author*

Abstract: This paper establishes a kinematic model of the pantograph based on Cartesian coordinates. On this basis, the dynamic model of the pantograph is derived using the first-kind Lagrange equations. Combined with the derived constraint equations, the dynamic characteristic equations of the pantograph are solved by numerical analysis. The derived kinematic and dynamic characteristic equations are applied to the structural analysis and optimization of pantographs for trunk railways and urban rail transit, providing theoretical support for pantograph design. Taking a typical metro pantograph as an example, the dynamic characteristic equations are solved, yielding the following conclusions: the motion trajectory of the panhead follows an "S" shape distribution; formulas for the lifting force, panhead displacement, and static contact force are obtained; significant vibration occurs between the panhead and the upper frame during the lifting and lowering process; and the natural frequency of the pantograph is 7.6 Hz.

Keywords: Pantograph; Kinematics; Dynamics; Cartesian Coordinates

1. Introduction

The pantograph is a current collection device installed on the upper part of electric trains. It works in conjunction with the overhead contact line to complete the function of electrical energy transmission. Kinematic analysis of the pantograph is an important method for designing its geometric parameters, while dynamic analysis is the foundation and prerequisite for studying pantograph-catenary coupled vibration.

Many scholars domestically and internationally have conducted research on the kinematics and dynamics of pantographs. Literature [1] lists the geometric constraint equations of the pantograph and uses ADAMS for dynamic simulation, providing the relationship between geometric parameters and kinematic evaluation parameters. Literature [2] uses vector dynamics methods to establish a kinematic model of the pantograph and solves the mathematical equation set via Simulink. Literature [3] takes the DSA series pantograph as an example, proposes a mechanical model considering the planar motion of the slide plate and stent and provides the differential equations of motion for the pantograph. Literature [4] establishes a geometric relationship model of the pantograph frame structure, uses the panhead motion as the optimization target, and applies single-objective optimization technology to optimize the geometric parameters of the Schunk-type pantograph. Literature [5] uses the multi-body dynamics software Simpack to establish a three-dimensional dynamic model of the pantograph, analyzing panhead trajectory, lifting torque, and natural frequency. Literature [6-10] provides the geometric motion relationships of the pantograph, uses the second-kind Lagrange equations to establish the dynamic model of the pantograph, considers the double four-bar linkage and panhead swing, resulting in a relatively complex model. Literature [11-13] uses the first-kind Lagrange equations to establish the dynamic model of the CX-type pantograph, provides hinge analysis and data for the pantograph, and conducts joint pantograph-catenary dynamic simulation with a finite element model of the catenary, but these references do not provide the corresponding mathematical model.

In summary, this paper first derives the constraint equations of the pantograph to

establish the kinematic model, then derives the dynamic model using the first-kind Lagrange equations. The constraint equations connect the kinematic and dynamic analyses. Using numerical methods, the motion parameters and force parameters of the pantograph are obtained, providing theoretical support for the structural design and optimization of the pantograph.

2. Kinematic Modeling of Pantograph

Pantographs come in various types, but their main structures generally include the panhead, upper frame, lower arm rod, push rod, balance rod, base frame, and transmission mechanism. The pantograph is a typical double four-bar linkage structure. The base frame, lower arm rod, push rod, and upper frame constitute the first four-bar linkage. The lower arm rod, upper frame, balance rod, and panhead suspension constitute the second four-bar linkage. The second four-bar linkage ensures that the rotation angle of the panhead swings as little as possible in space, keeping the panhead level. The structure of the pantograph is spatially symmetrical and can be simplified into a planar physical model. To simplify the physical model of the pantograph, the panhead is assumed to be reduced to a particle with a rotation angle constraint, the second four-bar linkage structure is neglected, and the focus is on analyzing the mechanical characteristics of the frame part. The pantograph is equivalent to 4 bodies: the lower arm rod, push rod, upper frame, and panhead. A body-fixed coordinate system is established at the center of mass of each body. Each body has 3 degrees of freedom, totaling 12 degrees of freedom, as shown in Eq. (1). The rotation point of the lower arm rod is taken as the origin of the inertial coordinate system for the pantograph, and the relevant positive directions are defined, as shown in Fig. 1. According to the local method referenced in [14], the configuration constraint equations for kinematics are established, as shown in Eq. (6). Five vector equations (matrices are represented in bold below) constrain 10 degrees of freedom, where **r** is the absolute translation coordinate vector of the body-fixed frame, **A** is the direction cosine matrix, as shown in Eq. (8), **ρ** is the relative translation coordinate vector of a fixed point on the rigid body relative to the body-fixed frame. Additionally, there is an assumption that the rotation angle of the panhead has an absolute angle constraint, as shown in Eq. (7). The kinematic model of the pantograph has only 1 independent degree of freedom. Expanding Eq. (7) and combining the geometric dimensions of each body shown in Fig. 2, the displacement constraint equations are obtained as shown in Eq. (9). The hinge types and coordinates are listed in Table 1.

$$q = (q_1^T, q_2^T, q_3^T, q_4^T)^T \tag{1}$$

$$\boldsymbol{q}_i = (x_i(t), y_i(t), \phi_i(t))^T, i = 1,2,3,4 \tag{2}$$

$$\Phi^{J1} = \vec{r_1} + A^1 \overrightarrow{\rho_1^o} = 0 \tag{3}$$

$$\Phi^{J2} = \vec{r_2} + A^2 \overrightarrow{\rho_2^c} = 0 \tag{4}$$

$$\Phi^{J3} = \vec{r_2} + A^2 \overrightarrow{\rho_2^d} - (\vec{r_3} + A^3 \overrightarrow{\rho_3^e}) = 0 \tag{5}$$

$$\Phi^{J5} = \vec{r_3} + A^3 \overrightarrow{\rho_3^g} - (\vec{r_4} + A^4 \overrightarrow{\rho_4^p}) = 0 \tag{6}$$

$$\varphi^{a\phi 1} = \phi_4 = 0 \tag{7}$$

$$\boldsymbol{A}^i = \begin{bmatrix} \cos\phi_i & -\sin\phi_i \\ \sin\phi_i & \cos\phi_i \end{bmatrix} = 0, i = 1,2,3,4 \tag{8}$$

$$\begin{cases} \varphi_1 = x_1 + \frac{l_1}{2}\cos\phi_1 = 0 \\ \varphi_2 = y_1 + \frac{l_1}{2}\sin\phi_1 = 0 \\ \varphi_3 = x_2 + \frac{l_2}{2}\cos\phi_2 + d_1 = 0 \\ \varphi_4 = y_2 + \frac{l_2}{2}\sin\phi_2 + d_2 = 0 \\ \varphi_5 = x_2 - \frac{l_2}{2}\cos\phi_2 - x_3 + (l_3 + l_4)\cos\phi_3 - d_4\sin\phi_3 = 0 \\ \varphi_6 = y_2 - \frac{l_2}{2}\sin\phi_2 - y_3 + (l_3 + l_4)\sin\phi_3 + d_4\cos\phi_3 = 0 \\ \varphi_7 = x_1 - \frac{l_1}{2}\cos\phi_1 - x_3 + l_4\cos\phi_3 - d_5\sin\phi_3 = 0 \\ \varphi_8 = y_1 - \frac{l_1}{2}\sin\phi_1 - y_3 + l_4\sin\phi_3 + d_5\cos\phi_3 = 0 \\ \varphi_9 = x_3 + l_5\cos\phi_3 - x_4 = 0 \\ \varphi_{14} = y_3 + l_5\sin\phi_3 - y_4 + d_3 = 0 \\ \varphi_{10} = \phi_4 = 0 \end{cases} \tag{9}$$

$$\varphi^{D1} = \phi_1 - \phi_0 - \omega t = 0 \tag{10}$$

$$x_0^2 + y_0^2 = d_6^2, x_0 = d_6\cos(\phi_0 + \omega t - 0.5\pi) \tag{11}$$

Table 1. (Regular) Pantograph Hinge Types and Coordinates.

No.	type	body$B_\alpha(\alpha)$	body$B_\alpha(\overrightarrow{\rho_\alpha})$	body$B_\beta(\alpha)$	body$B_\beta(\overrightarrow{\rho_\alpha})$	Coordinates
1	r	1	$l_1/2$, 0			0, 0
2	r	2	$l_2/2$, 0			$-d_1$, $-d_2$
3	r	2	$-l_2/2$, 0	3	$-l_3$-l_4, $-d_4$	

4	r	1	$-l_1/2$, 0	3	$-l_4$, $-d_5$	
5	r	3	l_5, 0	4	0, $-d_3$	
6	$a\phi$	4	0, 0			0

The additional driving constraint method is used to solve the constraint equation set (9), forming a closed set of mathematical equations. Since the transmission mechanism of the pantograph acts on the lower arm rod, applying a force around the origin through the steel wire rope causes the lower arm rod to rotate, realizing the lifting and lowering of the pantograph. In kinematic analysis, it is assumed that the lower arm rod rotates at a constant angular velocity ω, as shown in Eq. (10). The relationship between the displacement of the steel wire rope's action point at coordinates (x_0, y_0) and the angular velocity is given by Eq. (11). Theoretically, the pantograph's motion position is determined by the displacement of the steel wire rope. Combining Eqs. (9) and (10), and given geometric parameters and angular velocity, the pantograph's displacement at different times is obtained. Differentiating Eqs. (9) and (10) with respect to time yields the corresponding velocity and acceleration constraint equations. Eqs. (9) and (10) form a set of nonlinear equations, which are solved numerically using the Newton-Raphson method.

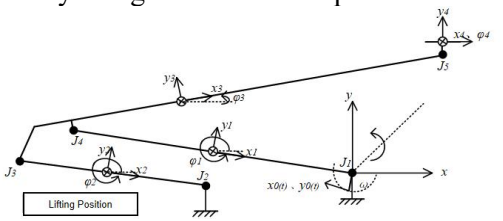

Figure 1. Kinematic Model of the Pantograph

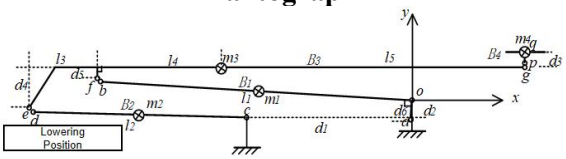

Figure 2. Schematic Diagram of Pantograph Geometric Parameters

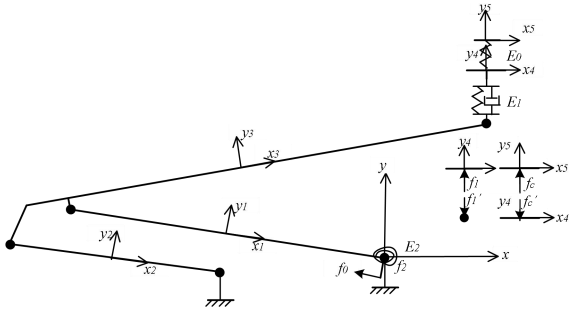

Figure 3. Constrained Dynamic Model of the Pantograph

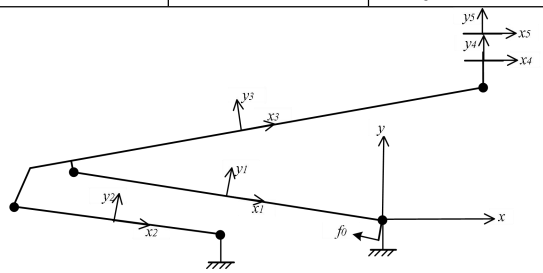

Figure 4. Static Model of the Pantograph

3. Dynamic Modeling of Pantograph

The kinematic model of the pantograph can provide the motion displacement, velocity, and acceleration at any time. The results of the kinematic model can be used as initial conditions for dynamics. However, the kinematic model does not consider the inertial effects of the pantograph and cannot fully describe its motion regularity over a certain period. Therefore, it is necessary to further establish the dynamic model of the pantograph.

The dynamic model of the pantograph needs to consider more mechanical characteristics. Based on the kinematic model, a linear spring-damper for the panhead suspension and a torsional spring-damper for the lower arm rod are added, as shown in Fig. 3. The forces on the pantograph consist of the external force f_0, internal forces f_1, f_1', and the inertial forces of the bodies. If the panhead in Fig. 3 were unconstrained, it would lift and lower freely under the drive of the lifting force f_0.

In reality, the pantograph operates within a certain height range, sliding in contact with the contact wire at a specific height. Therefore, the panhead is subject to the displacement constraint of the contact wire. Under the action of the lifting force, a contact force is generated between the panhead and the contact wire. In a static state, the static contact force between the pantograph and the contact wire at different heights should be constant: typically 70 N for national railways and 110 N for metros. Combining the actual operating conditions, the constrained dynamic model of the pantograph is established, as shown in Fig. 3. The number of bodies is increased to 5. The fifth body is assumed to be an exciter or the contact wire, and its inertial force is neglected (mass and inertia are very small). The fifth body and the panhead are connected by a force element,

representing the pantograph-catenary contact force f_c, f_c'. At this point, the dynamic model of the pantograph has 5 bodies and 15 degrees of freedom, as shown in Eq. (12). The dynamic equations of the pantograph are derived according to the first-kind Lagrange equations, as shown in Eq. (13), where Z represents the augmented mass matrix, Φq represents the Jacobian of the constraint equations, λ is the Lagrange multiplier related to the constraint forces, and Q represents the generalized force matrix. Analyzing the constrained pantograph model, it can be seen that the pantograph has only two independent degrees of freedom: one is the rotational degree of freedom of the lower arm rod, and the other is the vertical degree of freedom of the panhead. Therefore, there are 13 constraint equations. The J5 rotational hinge in the kinematic analysis should be changed to a relative position constraint hinge, only constraining the x-direction displacement between point g on the upper frame and point p on the panhead. Eq. (6) is rewritten as Eq. (15). At this point, the number of constraint equations is 10. Additionally, three more constraint equations are needed: the relative displacement constraint Eq. (16), the absolute angle constraint Eq. (17), and the driving displacement constraint Eq. (18). Combining constraint equations $\Phi^1$to Φ^{13}, the constraint equation set for the dynamic model of the pantograph is obtained as Eq. (19). Since Eq. (13) introduces 13 unknown Lagrange multipliers, 13 constraint equations Eq. (19) must be added. Because the form of Eq. (19) differs somewhat from the generalized acceleration matrix in Eq. (13), to abbreviate the matrix, Eq. (19) is differentiated twice with respect to time to obtain the acceleration matrix, as shown in Eq. (14). Eqs. (13) and (14) form a mathematically closed set of equations for the dynamic model of the pantograph. This equation set can be transformed into a set of first-order ordinary differential equations and solved numerically using linear algebra methods and ODE solvers. The specific solution method refers to literature [15]. The acceleration array γ in Eq. (13) is obtained from Eq. (20). The generalized forces are given by Eq. (21), where the force elements E_0, E_1, E_2 are given by Eq. (23). The direction of the lifting force is tangential to the circular motion with the origin as the center and d_6 as the radius. The initial conditions for solving the ODE are given by Eq. (24), where the displacement initial conditions need to add the driving displacement y_c based on the kinematics, and the velocity initial conditions are assumed to be 0.

$$\begin{aligned} &q' = (q_1^T, q_2^T, q_3^T, q_4^T, q_5^T)^T \\ &\boldsymbol{q}_i = (x_i(t), y_i(t), \phi_i(t))^T, i = 1,2,3,4,5 \end{aligned} \tag{12}$$

$$Z\ddot{q}' + \varphi_{q'}^T \lambda = \hat{F}^a \tag{13}$$

$$\varphi_{q'}\ddot{q}' = \gamma \tag{14}$$

$$\varphi^{ax1} = \begin{bmatrix} 1 & 0 \end{bmatrix} \cdot \varphi^{J5} = \varphi_9 = 0 \tag{15}$$

$$\varphi^{ax2} = x_5 - x_4 = \varphi_{11} = 0 \tag{16}$$

$$\varphi^{a\phi 2} = \phi_5 = \varphi_{12} = 0 \tag{17}$$

$$\varphi^{D2} = y_5 - y_c = \varphi_{13} = 0 \tag{18}$$

$$\varphi = \begin{pmatrix} \varphi_1 & \varphi_2 & \cdots & \varphi_{13} \end{pmatrix}^T = \mathbf{0} \tag{19}$$

$$\boldsymbol{\lambda} = \begin{pmatrix} \lambda_1 & \lambda_2 & \cdots & \lambda_{13} \end{pmatrix}^T \tag{20}$$

$$\gamma = -(\varphi_{q'}\dot{q}')_{q'}\dot{q}' - 2\varphi_{q't}\dot{q}' - \varphi_{tt} \tag{21}$$

$$\hat{\boldsymbol{F}}^a = \begin{bmatrix} -f_0\cos\phi_1 \\ -m_1 g - f_0\sin\phi_1 \\ -f_0 d_6 + f_2 \\ 0 \\ -m_2 g \\ 0 \\ 0 \\ -m_3 g + f_1' \\ f_1' l_5 \cos\phi_3 \\ 0 \\ -m_4 g + f_1 + f_c' \\ 0 \\ 0 \\ f_c \\ 0 \end{bmatrix} \tag{22}$$

$$\begin{cases} f_1 = -f_1' = -k_1(y_4 - (y_3 + l_5\sin\phi_3) - \mu_1) \\ \qquad -c_1(\dot{y}_4 - (\dot{y}_3 + l_5\dot{\phi}_3\cos\phi_3)) \\ f_2 = -c_2\dot{\phi}_1 \end{cases} \tag{23}$$

$$t = t_0, \boldsymbol{q}_0'(t_0) = \begin{bmatrix} \boldsymbol{q_0} \\ 0 \\ y_{c0} \\ 0 \end{bmatrix}, \dot{\boldsymbol{q}}_0'(t_0) = \mathbf{0} \tag{24}$$

$$\varphi_{q'}^T \lambda = \hat{F}^a \tag{25}$$

$$\varphi_u^T \lambda = \hat{F}_u^a \tag{26}$$

$$\varphi_w^T \lambda = \hat{F}_w^a \tag{27}$$

$$\lambda = \varphi_u^{-1T} \hat{F}_u^a \tag{28}$$

$$(\varphi_u^{-1}\varphi_w)^T \hat{F}_u^a - \hat{F}_w^a = 0 \tag{29}$$

Since the pantograph is a constrained structure,

it has an equilibrium state. It is necessary to calculate the static equilibrium position of the pantograph and the active forces and ideal constraint forces in the equilibrium state, such as studying the relationship between the lifting force and the static contact force. When in static equilibrium, the pantograph has no velocity or acceleration. Eq. (13) can be rewritten as Eq. (25). Using the LU decomposition condensation method, the **Φq** matrix is decomposed into the Jacobian of the independent variable array **w** and the Jacobian of the dependent variable array **u**, as shown in Eq. (26) and (27). Eq. (26) is rewritten as Eq. (28) and substituted into Eq. (27), obtaining the equation set without the Lagrange multiplier term, Eq. (29). Combined with Eq. (19), this forms the closed-form nonlinear algebraic equations for the static model of the pantograph.

In the dynamic model of the pantograph, there is one driving force and one driving displacement. The driving displacement is included in the constraint equations, and the driving force is in the generalized force matrix. Both are time variables. If both are constants, the dynamic equations can be simplified to static equations for solution. When calculating the static equilibrium problem of the pantograph, the force elements are equivalent to rigid connections, as shown in Fig. 4. At this point, the driving constraint y_5 differs from y_4 by μ_0. The panhead constraint force, i.e., the static contact force, can be obtained by calculating the Lagrange multiplier using Eq. (28).

Additionally, by removing the fifth body from Eqs. (13) and (14) and deleting the corresponding rows or columns in the matrices, the dynamic model of the pantograph for free lifting and lowering can be derived.

4. Example Analysis

Taking a typical pantograph commonly used in metros as an example, the above method is used to study the motion and forces of the pantograph. The geometric parameters of a typical metro pantograph are given in Table 2.

Table 2. Pantograph Geometric Parameters

Parameter	Value	Value	Parameter	Value
l1	1600	1180	l3	297
l4	578	1316	d1	723
d2	178	160	d4	170
d5	70	125	ϕ0	360

Note: Length unit is mm, angle unit is degree.

An important parameter in kinematic analysis is the motion trajectory of the panhead and the relationship between panhead motion and the lifting angle. Assuming the pantograph rises at an angular velocity ω = -1°/s, the horizontal and vertical displacement coordinates of the panhead are calculated, as shown in Fig. 5. It is found that as the panhead height increases, the horizontal displacement of the panhead first decreases, then increases, and then decreases again, forming an "S-shaped" motion, consistent with the trend in the example in literature [1]. The panhead has a horizontal displacement amplitude of 29.37 mm.

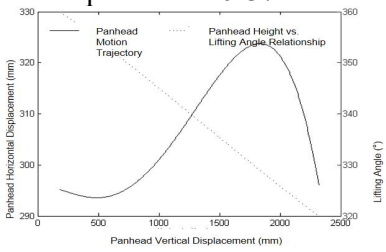

Figure 5. Panhead Motion vs. Lifting Angle

Using the geometric relationship obtained from the pantograph kinematic model analysis as the initial condition for the static and dynamic analysis of the pantograph, the static equilibrium state of the pantograph is analyzed. Table 3 provides the dynamic parameters of the pantograph. The panhead stiffness and damping in Table 3 are derived from the single-mass stiffness-damping vibration test of the panhead. The connection spring between body 5 and the panhead is calculated based on the contact stiffness given in EN50318. The rotational damping of the lower arm rod is assumed to be a small value.

Table 3. Pantograph Dynamic Parameters.

Parameter	Value	Parameter	Value	Parameter	Value
m1	19.37kg	m2	2.49kg	m3	9.29kg
m4	15.03kg	I1	7.77kgm-2	I2	0.41kgm-2
I3	5.37kgm-2	I4,I5	0.01kgm-2	m5	0.001kg
c1	5Ns/m	c2	10Ns/deg	μ1	m4g/k1
k0	50kN/m	μ0	0.1m	k1	30kN/m
m1	19.37kg	m2	2.49kg	m3	9.29kg

By adjusting the driving displacement y_5, the displacements of other components at a certain panhead working height are obtained. Applying the lifting force, the corresponding panhead constraint reaction force, i.e., the static contact force, is calculated. A set of lifting force and static contact force curves is calculated every 0.1 m in the range of 0.4 m to 1.4 m. Based on the calculation results, the relationship curves between lifting force and panhead vertical displacement are plotted, as shown in Fig. 6. It is found that with a constant output lifting force, the static contact force decreases as the lifting height increases; to maintain a constant static contact force, the lifting force must increase with the lifting height; a larger static contact force requires a larger lifting force. The data given in Fig. 6 is fitted with first-order polynomial curves, resulting in three linear fitting curves with very similar slopes. Observing the three curves, it is found that the vertical distances between the static contact forces are basically equal. Weighted averaging is performed on the fitted curves using lifting force, lifting height, and static contact force, resulting in Eq. (30), which is the calculation formula for the lifting force. Taking a typical metro pantograph as an example, the actual parameters in Eq. (30) are a_1=4782, a_2=16.8, a_3=1400. To maintain a constant static contact force at different panhead heights, the lifting force must vary.

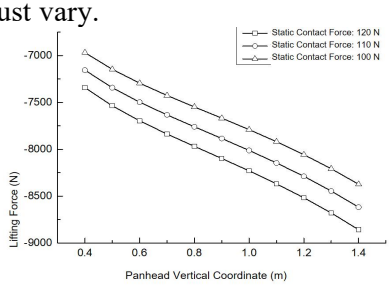

Figure 6. Relationship between Lifting Force and Panhead Vertical Displacement.

$$f_0 = -a_1 - a_2 f_c - a_3 y_4 \quad (30)$$

The dynamic model of the pantograph can be used to study the lifting and lowering process. Assuming the initial condition is the lowered position of the pantograph, and the lifting force is a step signal: constant force of -8700 N for the first 5 seconds, and constant force of -6500 N for the next 5 seconds, the accelerations of various components during pantograph lifting and lowering are studied. As shown in Fig. 7, it is found that the acceleration change of the panhead is the largest, followed by the acceleration change of the upper frame, while the changes of the lower arm rod and the push rod are very small, indicating that the main components affecting the dynamic performance of the pantograph are the panhead and the upper frame.

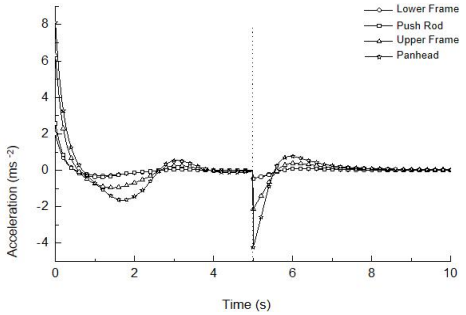

Figure 7. Acceleration Time History During Lifting and Lowering.

Finally, the inherent characteristics of the pantograph are studied. Taking the panhead vertical displacement of 1.4 m as the initial condition, the displacement y_5 is adjusted to output a constant amplitude of 0.01 m at frequencies from 0.1 to 20 Hz, studying the amplitude-frequency response of the pantograph at different frequencies. One calculation case corresponds to one frequency. Fig. 8 shows the variation curves of the vertical vibration displacement coordinates of various components with time under 7.6 Hz excitation. Fig. 9 shows the vibration amplitudes of various components versus frequency, i.e., the amplitude-frequency response. It is found that at 7.6 Hz, the vertical amplitudes of the pantograph components have extreme values. 7.6 Hz should be a natural frequency of this type of pantograph. The panhead has an inflection point at 0.15 Hz, while other components do not, so it is not considered a natural frequency. Theoretically, two independent degrees of freedom should have two natural frequencies, but one independent degree of freedom is the rotation of the lower arm rod, which has no spring, so the natural frequency there is infinitely close to 0.

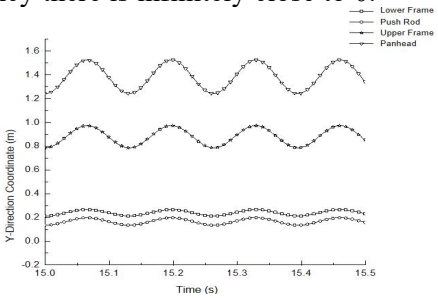

Figure 8. Amplitude Time History of Components under 7.6 Hz Excitation Displacement Frequency.

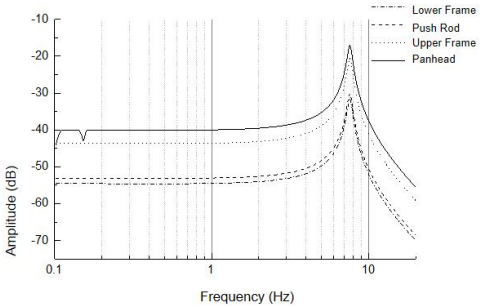

Figure 9. Amplitude-Frequency Response Curves of Components.

5. Conclusion

Based on Cartesian coordinates, the kinematic model of the pantograph is established, and the constraint equations are derived. The dynamic model of the pantograph is established using the first-kind Lagrange equations. Combined with the constraint equations, the system is solved through numerical methods. The kinematic and dynamic calculation method based on Cartesian coordinates can be applied to the structural analysis and optimization of pantographs for trunk railways and urban rail transit, providing theoretical support for pantograph design.

Using the above algorithm, the motion laws and mechanical performance of the pantograph are studied. Taking a typical metro pantograph as an example, the following results are obtained: the motion trajectory of the panhead follows an "S" shape distribution; calculation formulas for the lifting force, panhead displacement, and static contact force are derived; significant vibration occurs between the panhead and the upper frame during the lifting and lowering process; and the natural frequency of the pantograph is 7.6 Hz.

References

[1]Guilin Guo. Kinematics Analysis of High-speed Pantograph. Electric drive for locomotives. 2013,(5):13-16.

[2]Hang Han. Kinematic simulation of pantograph based on Simulink. Mechanical Research & Application. 2007,20(2):57-59.

[3]Min Li. Mechanical models and differential equations of motion for high speed pantographs. Journal of railway science and engineering. 2005, 2(3):83-87.

[4]Hongjiao Liu. Optimization of geometric parameters for high-speed pantograph mechanism. Journal of the china railway society. 2001,23(6):16-20.

[5]Kang Chen. Study of 3D Multi-body Dynamics Model of Pantograph for Electric Locomotive. Electric drive for locomotives. 2006,(5):11-14.

[6]Weihua Zhang. A Dynamic Analysis of The Pantograph. Journal of the china railway society. 1993,15(1):23-29.

[7]Guo-lei Ma. Research on pantograph system. Southwest Jiaotong University, 2009:10-25.

[8]Guiming Mei. The Dynamic Study of Pantograph Catenary System. Southwest Jiaotong University. 2010: 9-16.

[9]Huawei Wang. Pantograph System Analysis and Simulation Study Based on Multibody Dynamics. ZHEJIANG UNIVERSITY. 2010:18-36.

[10]Xianming Chen. The Design and Research of High Speed Pantograph V500. Southwest Jiaotong University. 2014:51-55.

[11]J. Pombo. Environmental and track perturbations on multiple pantograph interaction with catenaries in high-speed trains [J]. Computers and Structures .2013, 124:88--101.

[12]J.Ambrósio. Recent Developments in Pantograph Catenary Interaction Modelling and Analysis[J]. International Journal of Railway Technology. 2012, 1(1):249-278.

[13]J.Pombo. Multiple Pantograph Interaction With Catenaries in High-Speed Trains [J]. Journal of Computational and Nonlinear Dynamics. 2012, 7:041008-1-7.

[14]Jiazhen Hong. Theoretical Mechanics. Higher Education Press. 2008:182-186.

[15]Jiazhen Hong. Computational Dynamics of Multibody Systems. Higher Education Press. 1999:308-319.